Published in final edited form as:
Biochem Biophys Res Commun. 2010 July 23; 398(2): 272–277. doi:10.1016/j.bbrc.2010.06.077.

Characteristics of the Rat Cardiac Sphingolipid Pool in Two Mitochondrial Subpopulations

Jeffrey S. Monette[1,2], **Luis A. Gómez**[1,2], **Régis F. Moreau**[1,2], **Brett A. Bemer**[1], **Alan W. Taylor**[1], and **Tory M. Hagen**[1,2]

[1] Linus Pauling Institute, Oregon State University, Corvallis, OR 97331, USA

[2] Department of Biochemistry and Biophysics, Oregon State University, Corvallis, OR 97331, USA

Abstract

Mitochondrial sphingolipids play a diverse role in normal cardiac function and diseases, yet a precise quantification of cardiac mitochondrial sphingolipids has never been performed. Therefore, rat heart interfibrillary (IFM) and subsarcolemmal (SSM) mitochondria were isolated, lipids extracted, and sphingolipids quantified by LC-tandem mass spectrometry. Results showed that sphingomyelin (~10,000 pmols/mg protein) was the predominant sphingolipid regardless of mitochondrial subpopulation, and measurable amounts of ceramide (~70 pmols/mg protein) sphingosine, and sphinganine were also found in IFM and SSM. Both mitochondrial populations contained similar quantities of sphingolipids except for ceramide which was much higher in SSM. Analysis of sphingolipid isoforms revealed ten different sphingomyelins and six ceramides that differed from 16 to 24 carbon units in their acyl side-chains. Sub-fractionation experiments further showed that sphingolipids are a constituent part of the inner mitochondrial membrane. Furthermore, inner membrane ceramide levels were 32% lower versus whole mitochondria (45 pmols/mg protein). Three ceramide isotypes (C_{20}-, C_{22}-, and C_{24}-ceramide) accounted for the lower amounts. The concentrations of the ceramides present in the inner membranes of SSM and IFM differed greatly. Overall, mitochondrial sphingolipid content reflected levels seen in cardiac tissue, but the specific ceramide distribution distinguished IFM and SSM from each other.

Supplementary Key Words

ceramide; sphingomyelin; sphingosine; sphinganine; LC-mass spectroscopy

Introduction

Sphingolipids are a diverse class of lipids that collectively play important roles in membrane ordering reactions, signal transduction, and cell recognition [1;2]. These compounds consist of a sphingosine backbone linked to a fatty acyl side-chain of varying lengths. Subclasses of sphingolipids are further structurally categorized by different head-groups attached to the long-chain base. Metabolically, different sphingolipids often have opposing actions on cell function [3]. For instance, ceramide (e.g. *N*-acylsphingosine) promotes cell differentiation

Correspondence: Tory M. Hagen, 571 Weniger Hall, Linus Pauling Institute, Oregon State University, Corvallis, OR 97331, tory.hagen@oregonstate.edu, Phone: (541) 737-5083, Fax: (541) 737-5077.

and growth arrest and is considered as an integral part of apoptosis initiation [4]. In contrast, an increased level of sphingosine-1-phosphate tends to induce cellular proliferation and survival [5]. Thus, altering levels of a particular sphingolipid subclass relative to another often has significant effects on cell and tissue metabolism [6;7].

Mitochondria, key organelles involved in cellular bioenergetics and regulation of apoptosis [8], also appear to be important sub-cellular sites for sphingolipid action [9;10]. Both inner and outer mitochondrial membranes contain sphingomyelinases with neutral and acidic pH optima [6;11], and ceramidases have also been detected in mitochondrial-enriched fractions [12].

In concert with these enzymes, mitochondrial membranes normally contain a variety of sphingolipids. For example, mitochondria from brain, heart, and liver have discernable levels of ceramide [13] and sphingomyelin [14]. Additionally, in one of the most complete studies to date, Ardail et al. showed that rat liver mitochondria contain 3-ketosphinganine, sphinganine, and a variety of ceramide isoforms differing in acyl side-chain length [15]. This latter attribute may be important as different side-chains confer specific and sometimes opposing biological actions on sphingolipids [3]. Thus, mitochondria appear competent to metabolize at least certain sphingolipids and may therefore be responsive to external stimuli that could affect sphingolipid pools within the organelle.

In vitro studies also show that altering mitochondrial sphingolipid levels markedly affect organelle function. Addition of ceramides composed of certain acyl side-chains (e.g. C_{16}-ceramide) to mitoplasts results in inhibition of Complex IV [16], and induction of reactive oxygen species (ROS) [16;17]. Furthermore, accumulation of mitochondrial ceramides promotes apoptogenesis by causing dephosphorylation of Bcl-2 family heterodimers [18;19]. Alternatively, sphingosine-1-phosphate protects cells from mitochondrial-driven apoptosis [20]. These examples highlight the concept that altering the mitochondrial sphingolipid pool significantly affects both cellular bioenergetics and the propensity for programmed cell death. However, even though it appears that certain sphingolipids are constituents of mitochondrial membranes and can affect their function, a precise analysis of the overall mitochondrial sphingolipid pool has not been fully achieved.

The current study was undertaken to provide a more thorough characterization of the mitochondrial sphingolipid pool using LC-tandem mass spectrometry (LC/MS/MS). Cardiac mitochondria were chosen for this analysis because the heart contains two unique mitochondrial subpopulations that are either located along the myofibrils (interfibrillary [IFM]) or adjacent to the sarcoplasmic reticulum (subsarcolemmal [SSM]) [21]. Differences with respect to respiratory activity, propensity for oxidative damage, and their contribution to pathophysiologies have been reported for these two mitochondrial subpopulations [22;23]. As sphingolipids may theoretically be involved in the divergent functional properties of the IFM and SSM, the current study was intended to not only understand cardiac mitochondrial sphingolipids *per se*, but also to discern potential differences in sphingolipid content and composition in IFM and SSM.

Materials and Methods

Reagents

The following reagents were used: genistein, Triton X-100, and Tween 20 (Sigma-Aldrich, St. Louis, MO); subtilisin A (type VIII) and bovine serum albumin (EMD Biosciences, La Jolla, CA); and digitonin (Thermo Fisher Scientific, Pittsburg, PA). Purified sphingolipid standards were purchased from Avanti Polar Lipids (Alabaster, AL). Rabbit polyclonal antibody to the voltage-dependent anion channel protein (VDAC) and mouse monoclonal

antibody to protein disulfide isomerase (PDI) were purchased from Abcam, Inc (Cambridge, MA).

Ethical treatment of vertebrate animals

Fischer 344 rats (male, 4–6 months old) were obtained from the National Institute on Aging animal colonies. Animals were housed in approved facilities and maintained by the Department of Laboratory Animal Resources and Care, OSU. All animal procedures were performed in accordance with OSU guidelines for animal experimentation.

Mitochondrial and microsome isolation

Cardiac mitochondria were isolated using differential centrifugation and a brief protease digestion as previously described [21]. One noted change from this method is the use of subtilisin A instead of nagarse to release mitochondria from the myofibrils. Microsomes were obtained by subjecting the supernatant from the SSM isolation to centrifugation at 100,000 × g for one hour. All steps of the isolation were performed on ice or at 4°C. Protein values were determined using the BCA protein assay kit.

Mitochondrial inner membrane isolation

The outer mitochondrial membrane was selectively removed using digitonin [24]. Six mg/ml digitoninin at 37°C in isotonic buffer (225 mM mannitol, 75 mM sucrose, 10 mM KCl, 10 mM tris-HCl, 5 mM KH_2PO_4, pH 7.2) was determined to be optimal for removing outer membranes (Figure 1C). This procedure resulted in a highly purified inner mitochondrial membrane (IMM) fraction with less than 2% contamination of the outer membrane. The IMM could not be further purified by Percoll density centrifugation as yields were too low to allow LC/MS/MS analysis.

Assessment of mitochondrial purity

Sphingolipids are found in all cell membranes; therefore, it was necessary to determine the extent of non-mitochondrial membrane contamination in IFM and SSM. The levels of microsomes and lysosomes in the mitochondrial preparations were chosen for the assessment because they are the most likely sources of contamination for any cardiac mitochondrial isolation scheme [2]. Results showed that the extent of ER contamination was minimal as shown by the lack of PDI, a marker protein for the ER (Figure 1A). Similarly, mitochondrial contamination with lysosomes, as measured by N-acetyl-β-D-glucosaminidase (NAG) activity, was limited to ≤ 1.5% of that found in tissue homogenates (Figure 1B). These results, along with rigorous purification of the IMM from isolated mitochondrial subpopulations (Figure 1C), indicate that cardiac mitochondria and their isolated inner membranes were sufficiently free of extra-mitochondrial contaminants to properly assess sphingolipid content. However, outer mitochondrial membranes were found to be of insufficient purity to properly monitor sphingolipids. Thus, only the sphingolipid profile from IMM or intact mitochondria could be reported.

Western blotting

Western blotting was performed as detailed in Petersen Shay et al. [25].

Phospholipid phosphate determination

The amount of phospholipid phosphate was determined using a colorimetric assay developed by Bartlett et al. [26].

Lipid extraction

All samples were prepared as in Sullards and Merrill Jr. [27] with the exception that samples were not digested in KOH. Briefly, a sphingolipid internal standard (25 μl) was added to mitochondria (1 mg protein). Lipids were extracted with 1.5 ml of chloroform:methanol (1:2). After an overnight incubation at 48ºC, phases were separated by adding chloroform (2 ml) and H_2O (4 ml). The chloroform layer was aspirated and dried under N_2. The sample was reconstituted in 200 μl chloroform:methanol (3:1) and diluted 1:4 with acetonitrile:methanol:acetic acid (97:2:1) containing 5 mM ammonium acetate. Recovery of lipids was monitored by LC/MS/MS (see below); all sphingolipids of the internal standard were detected in quantifiable and reproducible amounts.

LC-Tandem mass spectrometry

Lipids were separated using a Shimadzu HPLC and a Supelco Discovery column (2 mm × 50 mm). The flow rate was set at 300 μl per minute. Mobile phase (A) contained methanol:water (60:40) while mobile phase (B) was composed of methanol:chloroform (60:40). Both solvents contained 0.2% (v/v) formic acid and 10 mM ammonium acetate. The column was pre-equilibrated at 100% (A) followed by a sample injection. The solvent was maintained at 100% (A) for one minute, followed by a linear gradient to 40% (B) after 8.0 minutes. Finally, the solvent mix was brought to 70% (B) after 13 minutes and then maintained at this percentage for the remainder of the 20 minute run.

The HPLC system was coupled through a TurboIon Spray source to a triple-quadrupole mass spectrometer operated in positive mode (Applied Biosystems/MDS Sciex, API 3000). Analytes were detected using Multiple Reaction Monitoring (MRM), which selectively detects fragment ions from the collision-induced dissociation (CID) of the parent molecular ion. Please see Supplemental Table I for a list of molecular ions and CID transitions. Quantification was based on comparison to sphingolipid standards.

Statistics

Data are presented as mean ± SEM. Samples were assessed for statistical significance using Student's t test. A p value <0.05 was considered statistically significant.

Results and Discussion

Analysis of rat heart sphingolipids

IFM and SSM sphingolipid profiles—Mitochondrial sphingolipids were monitored using LC/MS/MS and quantified according to Leibisch *et al.* [28]. Sphingomyelin was the predominant sphingolipid (10,000 pmols/mg protein) in cardiac IFM and SSM (Figure 2A). While ceramide (Figure 2B), sphingosine (Figure 2C), and sphinganine (Figure 2D) were measurable, these sphingolipids were at least 150-fold lower than sphingomyelin levels. Cardiac IFM and SSM thus contain similar quantities of each sphingolipid sub-class, which suggests that differences in their general sphingolipid profiles are not likely responsible for the functional divergence between these two mitochondrial subpopulations. In addition to these aforementioned sphingolipids, attempts were made to quantify sphingosine-1-phosphate, sphinganine-1-phosphate, as well as glucosylceramides in both IFM and SSM. However, while detectable in limited quantities, all fell below the quantitative limit of our assay. Thus, SSM and IFM primarily contain sphingomyelin and ceramide with minor amounts of other sphingolipids.

Comparison of mitochondrial sphingolipids to other cardiac membranes—In order to place the mitochondrial sphingolipid profile in context to other cardiac membranes,

sphingolipids were measured in lipid extracts from heart tissue and isolated microsomes. Figure 2 shows that mitochondrial sphingolipid content generally reflects the sphingolipid profile in cardiac tissue, but is noticeably lower relative to the levels seen in microsomes. Thus, even though mitochondria often form contiguous networks with the ER [29], the relatively low levels of mitochondrial sphingolipids suggest that lateral diffusion from the ER is not the sole means of regulating mitochondrial sphingolipid levels.

Sphingolipids of the inner mitochondrial membrane—Because the IMM is relatively impervious to proton and solute translocation, we hypothesized that sphingolipids, which participate in membrane ordering, may be components of this specialized membrane [30]. Determination of sphingolipid subclasses revealed that inner membranes of both IFM and SSM contained sphingomyelin, ceramide, sphingosine and sphinganine (Figure 2). While this profile was similar to intact mitochondria, IMM were markedly enriched in sphingomyelin versus whole mitochondria. This relative enrichment was observed for both SSM and IFM inner membranes, which were 58% and 64% higher, respectively.

Large differences in ceramide levels between IFM and SSM inner membranes were observed (Figure 2B). SSM inner membrane ceramides were elevated at least 3-fold relative to the IFM (Figure 2B), suggesting potential ceramide-specific characteristics in the SSM. While not currently examined, it is known that elevated ceramides inhibit the respiratory chain [16], which indicates that higher SSM ceramide levels may be a factor in the lower rates of respiratory activity evident for this subpopulation [21]. Further work will be necessary to define the potential functional consequences of the asymmetric distribution of ceramides in IFM and SSM inner membranes.

Quantification of mitochondrial sphingolipid isoforms

A significant advantage of using LC/MS/MS is the opportunity to monitor not only a particular sphingolipid class, but also the distribution of sphingolipid isotypes based on acyl side-chain length. Analysis of specific sphingolipid species revealed that rat cardiac mitochondria contain numerous isoforms differing in side-chain unsaturation and acyl chain length (16–24 carbons).

Specific sphingomyelin isoforms in cardiac mitochondria—As shown in Table I, no discernable differences in sphingomyelins were evident between the mitochondrial subpopulations. C_{20}- and C_{22}-sphingomyelin were the predominant mitochondrial isotypes, each of which comprised approximately 33% of the total sphingomyelin pool. As with the general sphingomyelin profile (Figure 2), the distribution patterns of specific sphingomyelin isoforms generally reflect that seen for cardiac tissue, and not for microsomes (Table I). Purified cardiac mitochondria contain low amounts of C_{16}-, C_{18}-, and C_{24}-sphingomyelin when compared to microsomes. The limited levels of these sphingomyelins are notable because ceramides with similar acyl side-chains accumulate during stress insult [31;32]. Thus stress-activated sphingomyelinase production of ceramide may not be the sole route of ceramide elevation in mitochondria, which could implicate extra-mitochondrial transfer [33].

Specific ceramide isoforms in cardiac mitochondria—Distinct differences in ceramide isoform patterns were evident when compared to the mitochondrial sphingomyelin profile (Figure 3). Regardless of subpopulation, mitochondria contain six ceramides having acyl chain lengths that range from 16- to 24-carbon units (Figure 3 and Table I). As opposed to the sphingomyelins which had five unsaturated species, the ceramide pool contained only one isoform ($C_{24:1}$-ceramide) with a site of unsaturation (Figure 3). The general profile of mitochondrial ceramide is similar to that found in brain [34] and liver [15]; however, the

absolute amounts of a particular ceramide isotype are different between cardiac mitochondria and mitochondria from other organs [15;34].

In terms of ceramide distribution, C_{24}-ceramide is the most abundant mitochondrial ceramide (~40%) in both IFM and SMM, while C_{16}- and C_{18}-ceramide are the most limited (Figure 3A). IFM and SSM contain similar amounts of C_{16}- and C_{18}-ceramide but all other species are higher in the IFM as compared to the SSM (>50%, $P < 0.05$).

Ceramide isoforms in IFM and SSM inner membranes—Analysis of inner membrane ceramides showed that both IFM and SSM contained all 6 isotypes that were present in intact mitochondria. However, overall, inner membrane ceramide levels and the amount of a particular ceramide varied markedly between IFM and SSM. As shown in Figure 2B, the SSM inner membrane contained significantly higher ceramide levels than intact mitochondria. This enrichment stemmed from elevated levels of all six ceramide species (Figure 3B). In particular, C_{16}- and C_{18}-ceramide were 21- and 9-fold higher, respectively, in the inner membrane than corresponding levels in the intact SSM. Also, all other ceramide isoforms were at least 2-fold higher than whole SSM.

When comparing ceramides in intact mitochondria with the inner membrane fraction, it was found that the IFM inner membrane is enriched in C_{16}- and C_{18}-ceramide, while being limited in ceramides with longer acyl chain lengths (Figure 3C). This apparent ceramide isoform asymmetry in mitochondrial membranes was independent of protein content, as a similar distribution pattern was also observed when based on phospholipid phosphate levels in lieu of protein amounts (Supplemental Figure 1).

IFM inner membrane ceramide isotypes were generally less abundant versus the intact organelle (Figure 3D). For example, C_{16}-ceramide was approximately 50% of the total; only C_{18}-ceramide values in the inner membrane approached that of intact IFM (Figure 3D). The tissue as a whole shared a similar profile to that of both the SSM and IFM, and hence was distinct from the inner membrane patterns. The microsomal ceramide pool contained the same acyl side-chains as the mitochondria and tissue but all isotypes were found at relatively high levels. Also, the amounts of each ceramide isotype relative to one another were different than those found in tissue and intact mitochondria (Figure 3D). These results once again indicate that microsomal sphingolipids are a distinct pool from the mitochondria.

Conclusions

Given the critical role that these lipids play in mitochondrial function, it is important to understand the general composition and membrane distribution of cardiac mitochondrial sphingolipids. The present work shows that cardiac mitochondria contain an array of sphingolipids, which reflects the distribution seen in heart and other tissues [15;34]. Despite this resemblance, the concentration of a given mitochondrial sphingolipid isotype varies widely and depends on the tissue studied. For example, liver mitochondria predominantly contain C_{16}-, C_{18}-, $C_{18:1}$-ceramide with C_{24}-ceramide being a minor constituent; C_{22}-ceramide is not detected [15]. In contrast, we report that C_{24}- and C_{22}-ceramide are the most abundant ceramides found in cardiac mitochondria. The reason(s) for these differences are not presently known, but may be due to tissue specific expression of ceramide synthases [35], which would significantly influence composition of mitochondrial ceramide isotypes in a particular organ.

The functional consequences for different ceramides in mitochondria have yet to be explored. However, the relative abundance of a ceramide species may modulate the sensitivity of mitochondria to apoptotic stimuli [3] or affect ROS production. Thus, a post-mitotic organ such as the heart may limit shorter-chain ceramides to modulate pro-apoptotic

signals versus a mitotically active organ like the liver, which can readily undergo tissue regeneration.

Sphingolipids play key roles in membrane curvature, regulation of energy production, and membrane permeability. Thus, alterations in basal sphingolipid levels may be the root-cause for the metabolic and structural differences found between SSM and IFM. Our results show that the sphingomyelin, sphingosine, and sphinganine content of cardiac mitochondria are nearly identical, and therefore cannot contribute to the functional differences of these two subpopulations. However, IFM and SSM display distinct ceramide profiles, which could contribute to differences in respiratory characteristics and sensitivity to pro-apoptotic stimuli. This in turn, may play a vital role in disease states, such as the decline in cardiac function seen in aging, where IFM becomes specifically dysfunctional.

We are currently attempting to determine both the mechanism(s) causing IFM and SSM ceramide asymmetry, and the functional consequences of such an asymmetry. With regards to the mechanism, the recent work by Wu et al. may be instructive, as this group showed that a novel isoform of neutral sphingomyelinase exists in mitochondria [36]. This presents the intriguing possibility of a differential expression or regulation of neutral sphingomyelinase in IFM and SSM. Thus, ceramide pool sizes and specific isoforms could be regulated via the catabolism of sphingomyelin to ceramide.

Supplementary Material

Refer to Web version on PubMed Central for supplementary material.

Acknowledgments

The authors would like to thank Judy Butler, Eric Smith, and Alexander Michels, Ph.D., for careful reading of the manuscript. The research was funded by the National Institute on Aging, grant number 2R01AG017141. We also acknowledge the facilities service core of the NIEHS (NIEHS ES00240).

Abbreviations

SSM	subsarcolemmal mitochondria
IFM	interfibrillary mitochondria
MRM	multiple reaction monitoring
CID	collision induced dissociation
ER	endoplasmic reticulum
ROS	reactive oxygen species
VDAC	voltage-dependent anion channel protein
PDI	protein disulfide isomerase
LC/MS/MS	LC-tandem mass spectrometry
NAG	N-acetyl-β-D-glucosaminidase
IMM	inner mitochondrial membrane

References

1. Goni FM, Alonso A. Biophysics of sphingolipids I. Membrane properties of sphingosine, ceramides and other simple sphingolipids. Biochim Biophys Acta. 2006; 1758:1902–21. [PubMed: 17070498]

2. Futerman AH, Hannun YA. The complex life of simple sphingolipids. EMBO Rep. 2004; 5:777–82. [PubMed: 15289826]
3. Senkal CE, Ponnusamy S, Bielawski J, Hannun YA, Ogretmen B. Antiapoptotic roles of ceramide-synthase-6-generated C16-ceramide via selective regulation of the ATF6/CHOP arm of ER-stress-response pathways. FASEB J. 24:296–308. [PubMed: 19723703]
4. Hannun YA, Obeid LM. The Ceramide-centric universe of lipid-mediated cell regulation: stress encounters of the lipid kind. J Biol Chem. 2002; 277:25847–50. [PubMed: 12011103]
5. Cuvillier O, Pirianov G, Kleuser B, Vanek PG, Coso OA, Gutkind S, Spiegel S. Suppression of ceramide-mediated programmed cell death by sphingosine-1-phosphate. Nature. 1996; 381:800–3. [PubMed: 8657285]
6. Pettus BJ, Chalfant CE, Hannun YA. Ceramide in apoptosis: an overview and current perspectives. Biochim Biophys Acta. 2002; 1585:114–25. [PubMed: 12531544]
7. Luberto C, Kraveka JM, Hannun YA. Ceramide regulation of apoptosis versus differentiation: a walk on a fine line. Lessons from neurobiology. Neurochem Res. 2002; 27:609–17. [PubMed: 12374196]
8. Brenner D, Mak TW. Mitochondrial cell death effectors. Curr Opin Cell Biol. 2009; 21:871–7. [PubMed: 19822411]
9. Birbes H, El Bawab S, Obeid LM, Hannun YA. Mitochondria and ceramide: intertwined roles in regulation of apoptosis. Adv Enzyme Regul. 2002; 42:113–29. [PubMed: 12123710]
10. Kong JY, Rabkin SW. Mitochondrial effects with ceramide-induced cardiac apoptosis are different from those of palmitate. Arch Biochem Biophys. 2003; 412:196–206. [PubMed: 12667483]
11. Birbes H, El Bawab S, Hannun YA, Obeid LM. Selective hydrolysis of a mitochondrial pool of sphingomyelin induces apoptosis. Faseb J. 2001; 15:2669–79. [PubMed: 11726543]
12. Bionda C, Portoukalian J, Schmitt D, Rodriguez-Lafrasse C, Ardail D. Subcellular compartmentalization of ceramide metabolism: MAM (mitochondria-associated membrane) and/or mitochondria? Biochem J. 2004; 382:527–33. [PubMed: 15144238]
13. Basu R, Oudit GY, Wang X, Zhang L, Ussher JR, Lopaschuk GD, Kassiri Z. Type 1 diabetic cardiomyopathy in the Akita (Ins2WT/C96Y) mouse model is characterized by lipotoxicity and diastolic dysfunction with preserved systolic function. Am J Physiol Heart Circ Physiol. 2009; 297:H2096–108. [PubMed: 19801494]
14. Kiebish MA, Han X, Cheng H, Lunceford A, Clarke CF, Moon H, Chuang JH, Seyfried TN. Lipidomic analysis and electron transport chain activities in C57BL/6J mouse brain mitochondria. J Neurochem. 2008; 106:299–312. [PubMed: 18373617]
15. Ardail D, Popa I, Alcantara K, Pons A, Zanetta JP, Louisot P, Thomas L, Portoukalian J. Occurrence of ceramides and neutral glycolipids with unusual long-chain base composition in purified rat liver mitochondria. FEBS Lett. 2001; 488:160–4. [PubMed: 11163764]
16. Di Paola M, Cocco T, Lorusso M. Ceramide interaction with the respiratory chain of heart mitochondria. Biochemistry. 2000; 39:6660–8. [PubMed: 10828984]
17. Gudz TI, Tserng KY, Hoppel CL. Direct inhibition of mitochondrial respiratory chain complex III by cell-permeable ceramide. J Biol Chem. 1997; 272:24154–8. [PubMed: 9305864]
18. Novgorodov SA, Szulc ZM, Luberto C, Jones JA, Bielawski J, Bielawska A, Hannun YA, Obeid LM. Positively charged ceramide is a potent inducer of mitochondrial permeabilization. J Biol Chem. 2005; 280:16096–105. [PubMed: 15722351]
19. Ruvolo PP, Deng X, Ito T, Carr BK, May WS. Ceramide induces Bcl2 dephosphorylation via a mechanism involving mitochondrial PP2A. J Biol Chem. 1999; 274:20296–300. [PubMed: 10400650]
20. Agudo-Lopez A, Miguel BG, Fernandez I, Martinez AM. Involvement of mitochondria on neuroprotective effect of sphingosine-1-phosphate in cell death in an in vitro model of brain ischemia. Neurosci Lett. 470:130–3. [PubMed: 20045720]
21. Palmer JW, Tandler B, Hoppel CL. Biochemical properties of subsarcolemmal and interfibrillar mitochondria isolated from rat cardiac muscle. J Biol Chem. 1977; 252:8731–9. [PubMed: 925018]

22. Fannin SW, Lesnefsky EJ, Slabe TJ, Hassan MO, Hoppel CL. Aging selectively decreases oxidative capacity in rat heart interfibrillar mitochondria. Arch Biochem Biophys. 1999; 372:399–407. [PubMed: 10600182]
23. Suh JH, Heath SH, Hagen TM. Two subpopulations of mitochondria in the aging rat heart display heterogenous levels of oxidative stress. Free Radic Biol Med. 2003; 35:1064–72. [PubMed: 14572609]
24. Nair JR, McGuire JJ. Submitochondrial localization of the mitochondrial isoform of folylpolyglutamate synthetase in CCRF-CEM human T-lymphoblastic leukemia cells. Biochim Biophys Acta. 2005; 1746:38–44. [PubMed: 16169100]
25. Petersen Shay K, Hagen TM. Age-associated impairment of Akt phosphorylation in primary rat hepatocytes is remediated by alpha-lipoic acid through PI3 kinase, PTEN, and PP2A. Biogerontology. 2008
26. Bartlett GR. Phosphorus assay in column chromatography. J Biol Chem. 1959; 234:466–8. [PubMed: 13641241]
27. Merrill AH Jr, Sullards MC, Allegood JC, Kelly S, Wang E. Sphingolipidomics: high-throughput, structure-specific, and quantitative analysis of sphingolipids by liquid chromatography tandem mass spectrometry. Methods. 2005; 36:207–24. [PubMed: 15894491]
28. Liebisch G, Drobnik W, Reil M, Trumbach B, Arnecke R, Olgemoller B, Roscher A, Schmitz G. Quantitative measurement of different ceramide species from crude cellular extracts by electrospray ionization tandem mass spectrometry (ESI-MS/MS). J Lipid Res. 1999; 40:1539–46. [PubMed: 10428992]
29. Simmen T, Lynes EM, Gesson K, Thomas G. Oxidative protein folding in the endoplasmic reticulum: Tight links to the mitochondria-associated membrane (MAM). Biochim Biophys Acta.
30. Chiantia S, Kahya N, Ries J, Schwille P. Effects of ceramide on liquid-ordered domains investigated by simultaneous AFM and FCS. Biophys J. 2006; 90:4500–8. [PubMed: 16565041]
31. Jin J, Hou Q, Mullen TD, Zeidan YH, Bielawski J, Kraveka JM, Bielawska A, Obeid LM, Hannun YA, Hsu YT. Ceramide generated by sphingomyelin hydrolysis and the salvage pathway is involved in hypoxia/reoxygenation-induced Bax redistribution to mitochondria in NT-2 cells. J Biol Chem. 2008; 283:26509–17. [PubMed: 18676372]
32. Senkal CE, Ponnusamy S, Rossi MJ, Bialewski J, Sinha D, Jiang JC, Jazwinski SM, Hannun YA, Ogretmen B. Role of human longevity assurance gene 1 and C18-ceramide in chemotherapy-induced cell death in human head and neck squamous cell carcinomas. Mol Cancer Ther. 2007; 6:712–22. [PubMed: 17308067]
33. Kumagai K, Yasuda S, Okemoto K, Nishijima M, Kobayashi S, Hanada K. CERT mediates intermembrane transfer of various molecular species of ceramides. J Biol Chem. 2005; 280:6488–95. [PubMed: 15596449]
34. Yu J, Novgorodov SA, Chudakova D, Zhu H, Bielawska A, Bielawski J, Obeid LM, Kindy MS, Gudz TI. JNK3 signaling pathway activates ceramide synthase leading to mitochondrial dysfunction. J Biol Chem. 2007; 282:25940–9. [PubMed: 17609208]
35. Mizutani Y, Kihara A, Igarashi Y. Mammalian Lass6 and its related family members regulate synthesis of specific ceramides. Biochem J. 2005; 390:263–71. [PubMed: 15823095]
36. Wu BX, Rajagopalan V, Roddy PL, Clarke CJ, Hannun YA. Identification and characterization of murine mitochondria-associated neutral sphingomyelinase (MA-nSMase), the mammalian sphingomyelin phosphodiesterase 5. J Biol Chem. 285:17993–002. [PubMed: 20378533]

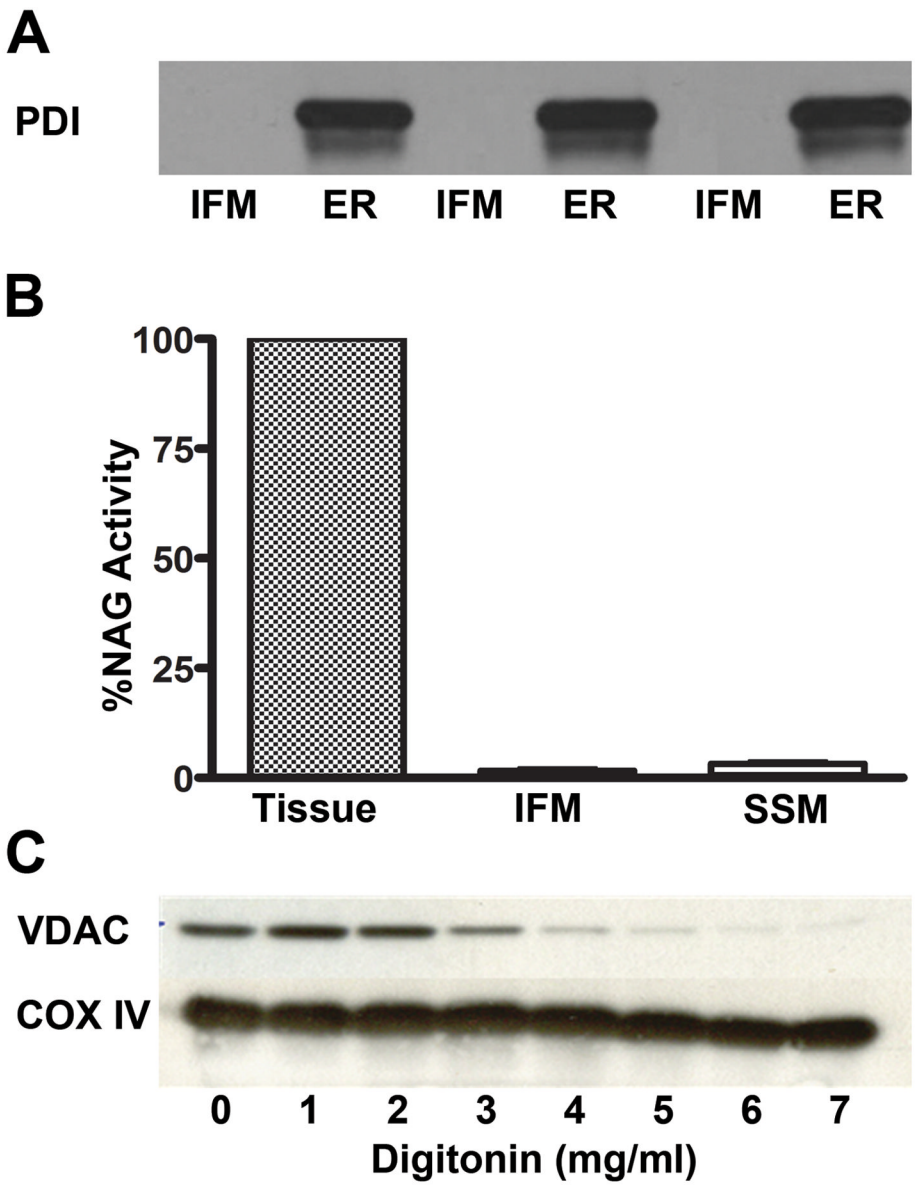

Figure 1. Intact mitochondria and inner membrane preparations are sufficiently pure for sphingolipid determination

Microsomal and lysosomal contamination of the IFM was monitored by measuring protein disulfide isomerase (PDI) and N-acetyl-β-D-glucosaminidase (NAG) activity, respectively. (A) Western blot analysis shows no detectable PDI in IFM preparations. n=3; (B) The percentage of NAG in IFM and SSM were ≤1.5% of that found in cardiac tissue homogenates. N=3; (C) Optimal digitonin levels to solubilize mitochondrial outer membranes from the IMM were determined. Western blot analysis showed successively greater removal of VDAC, a protein marker of mitochondrial outer membranes, with increasing digitonin levels added; however, COX IV (an inner membrane marker) remained constant regardless of digitonin levels. The blot shown is typical of four preparations.

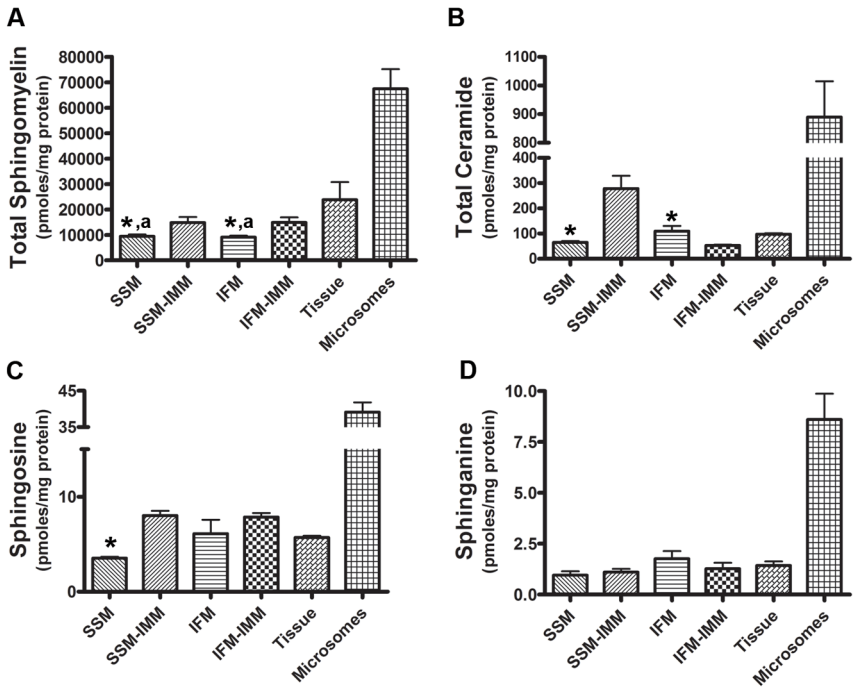

Figure 2. Sphingolipid profiles in mitochondrial and extra-mitochondrial cardiac membranes

Lipids extracted from IFM, SSM, or their respective inner membranes were subjected to LC-MS/MS and sphingolipids quantified relative to standards. Sphingolipids were also monitored in cardiac microsomes and lipid extracts from tissue homogenates. (A) Sphingomyelin; (B) ceramide; (C) sphingosine; and (D) sphinganine are shown. Data are Mean ± SEM, n=6; an asterisk (*) denotes significant differences between intact mitochondria and IMM; a superscript ([a]) indicates a statistically significant difference from whole tissue, $p < 0.05$.

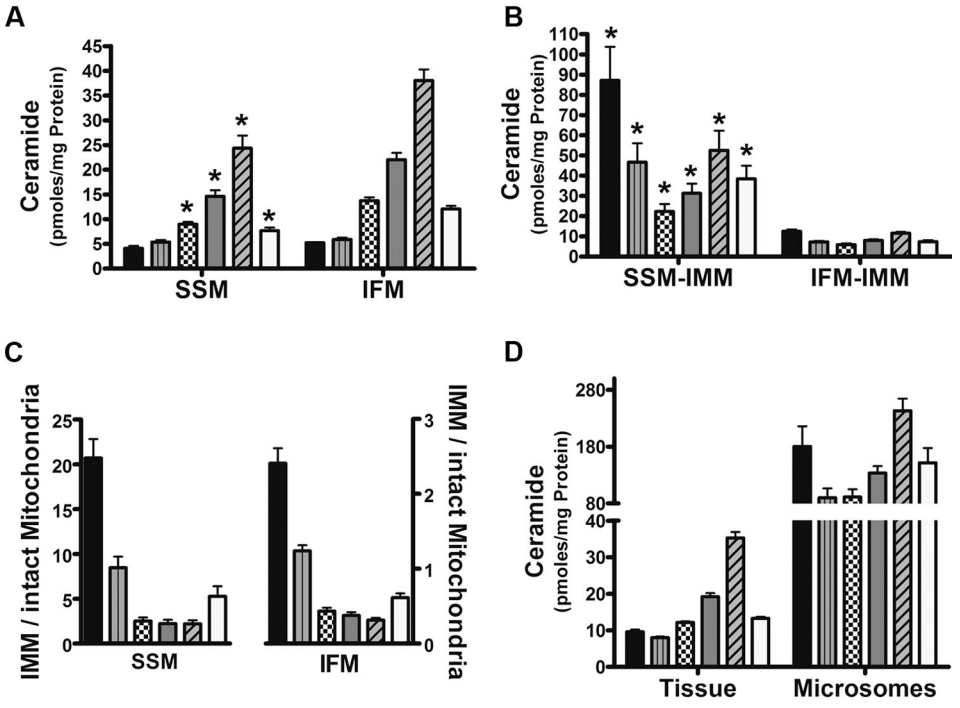

Figure 3. Ceramide isotypes in mitochondrial and extra-mitochondrial cardiac membranes

Ceramides were quantified in indicated cardiac membranes using LC/MS/MS. Results showed that all membranes contain six ceramide species with side chains from 16 to 24 carbons in length. (A) Ceramide distribution in SSM and IFM. (B) Profile of SSM and IFM ceramide isotypes in mitochondrial inner membranes. (C) Ratio of inner membrane ceramides to those of intact mitochondria. (D) Ceramide levels found in extra-mitochondrial membranes. Data represents the Mean ± SEM, n = 6; an asterisk (*) denotes a significant difference to the corresponding isotype in IFM, $p < 0.05$. Bars represent: C16-ceramide (black), C18-ceramide (gray vertical line), C20-ceramide (checkered), C22-ceramide (gray), C24-ceramide (angled line), and C24:1-ceramide (clear).

Biochem Biophys Res Commun. Author manuscript; available in PMC 2011 July 23.

Table 1

Sphingomyelin Content of various cardiac myocyte membranes.

	(pmols/mg protein)					
Sphingomyelin Species	**IFM**	**IFM-IMM**	**SSM**	**SSM-IMM**	**Tissue**	**Microsomes**
C_{16}-sphingomyelin	25 ± 4	907± 62	45 ± 12	1749 ± 400	1370 ± 88	11002 ± 872
C_{18}-sphingomyelin	51 ± 4	722 ± 70	64 ± 11	1039 ± 229	822 ± 76	6504 ± 381
C_{20}-sphingomeylin	3394 ± 216	4496 ± 670	3418 ± 281	4160± 761	7537 ± 2422	15530 ± 2153
C_{22}-sphingomyelin	3465 ± 203	4733 ± 594	3591 ± 315	4223 ± 680	8497 ± 2642	18514 ± 2523
C_{24}-sphingomyelin	161 ± 11	956 ± 90	124 ± 19	1035 ± 186	1155 ± 139	7476 ± 574
$C_{16:1}$-sphingomyelin	0.95 ± 0.04	17 ± 1.2	1.28 ± 0.22	25 ± 6	24 ± 1.3	192 ± 11
$C_{18:1}$-sphingomyelin	2.81 ± 0.31	81 ± 8.5	3.51 ± 0.59	76 ± 17	81 ± 6.5	695 ± 53
$C_{20:1}$-sphingomyelin	278 ± 71	457 ± 97	258± 67	341 ± 89	837 ± 336	1630 ± 270
$C_{22:1}$-sphingomyelin	1746 ± 142	2545 ± 394	1901± 128	2186 ± 429	3514 ± 1245	5923 ± 941
$C_{24:1}$-sphingomyelin	1020 ± 53	1695 ± 178	1158± 81	1861 ± 284	2368 ± 853	6395 ± 900